



# 1,2-Dichloroethane impairs glucose and lipid homeostasis in the livers of NIH Swiss mice



Ting Wang<sup>a,1</sup>, Dandan Xu<sup>a,1</sup>, Qiming Fan<sup>a</sup>, Weifeng Rong<sup>b</sup>, Jiewei Zheng<sup>b</sup>, Chen Gao<sup>a</sup>, Guoliang Li<sup>b</sup>, Ni Zeng<sup>a</sup>, Tao Guo<sup>a</sup>, Lihai Zeng<sup>b</sup>, Fei Wang<sup>a</sup>, Chen Xiao<sup>a</sup>, Li Cai<sup>a</sup>, Shangqing Tang<sup>a</sup>, Xinlei Deng<sup>a</sup>, Xiao Yin<sup>b</sup>, Manqi Huang<sup>b</sup>, Fengrong Lu<sup>b</sup>, Qiansheng Hu<sup>a</sup>, Wen Chen<sup>a</sup>, Zhenlie Huang<sup>b,\*\*</sup>, Qing Wang<sup>a,\*</sup>

<sup>a</sup> Faculty of Preventive Medicine, A Key Laboratory of Guangzhou Environmental Pollution and Risk Assessment, School of Public Health, Sun Yat-sen University, Guangzhou 510080, China

<sup>b</sup> Guangdong Provincial Key Laboratory of Occupational Disease Prevention and Treatment, Department of Toxicology, Guangdong Province Hospital for Occupational Disease Prevention and Treatment, Guangzhou 510300, China

## ARTICLE INFO

### Article history:

Received 21 November 2016  
Received in revised form 6 February 2017  
Accepted 7 February 2017  
Available online 8 February 2017

**Keywords:**  
1,2-Dichloroethane  
2-Chloroacetic acid  
Hepatotoxicity  
Glycogen  
Triglyceride

## ABSTRACT

Excessive exposure to 1,2-Dichloroethane (1,2-DCE), a chlorinated organic toxicant, can lead to liver dysfunction. To fully explore the mechanism of 1,2-DCE-induced hepatic abnormalities, 30 male National Institutes of Health (NIH) Swiss mice were exposed to 0, 350, or 700 mg/m<sup>3</sup> of 1,2-DCE, via inhalation, 6 h/day for 28 days. Increased liver/body weight ratios, as well as serum AST and serum ALT activity were observed in the 350 and 700 mg/m<sup>3</sup> 1,2-DCE exposure group mice, compared with the control group mice. In addition, decreased body weights were observed in mice exposed to 700 mg/m<sup>3</sup> 1,2-DCE, compared with control mice. Exposure to 350 and 700 mg/m<sup>3</sup> 1,2-DCE also led to significant accumulation of hepatic glycogen, free fatty acids (FFA) and triglycerides, elevation of blood triglyceride and FFA levels, and decreases in blood glucose levels. Results from microarray analysis indicated that the decreases in glucose-6-phosphatase catalytic subunit (G6PC) and liver glycogen phosphorylase (PYGL) expression, mediated by the activation of AKT serine/threonine kinase 1 (Akt1), might be responsible for the hepatic glycogen accumulation and steatosis. Further *in vitro* study demonstrated that 2-chloroacetic acid (1,2-DCE metabolite), rather than 1,2-DCE, up-regulated Akt1 phosphorylation and suppressed G6PC and PYGL expression, resulting in hepatocellular glycogen accumulation. These results suggest that hepatic glucose and lipid homeostasis are impaired by 1,2-DCE exposure via down-regulation of PYGL and G6PC expression, which may be primarily mediated by the 2-chloroacetic acid-activated Akt1 pathway.

© 2017 Elsevier B.V. All rights reserved.

## 1. Introduction

1,2-Dichloroethane (1,2-DCE), commonly known as ethylene dichloride (EDC), is a type of halogenated aliphatic hydrocarbon. In industry, 1,2-DCE is primarily used as an intermediate to make vinyl chloride, trichloroethylene, and perchloroethylene. In China,

it is extensively used as an organic solvent adhesive thinner. Furthermore, 1,2-DCE is also present in ambient air, groundwater, surface water, and drinking water (Chernichenko et al., 2009; Hou et al., 2012). It is a highly volatile liquid, thus the primary route of 1,2-DCE exposure for human beings is through vapor inhalation. After absorption, 1,2-DCE is quickly distributed and accumulates in organs rich in fat and lipids such as the brain, liver, kidney, spleen, and adipose tissue (Igwe et al., 1986; Take et al., 2014). During the past twenty years, 1,2-DCE poisoning has become one of the most severe occupational hazards in China (Liu et al., 2010; Chen et al., 2015a, 2015b; Zhou et al., 2015). According to reports, the concentration of 1,2-DCE in some workplaces can reach up to 500–1500 mg/m<sup>3</sup> (123.52–370.57 ppm), which is much higher

\* Corresponding author at: Faculty of Preventive Medicine, School of Public Health, Sun Yat-sen University, 74 Zhongshan Road 2, Guangzhou, 510080, China.

\*\* Corresponding author at: Department of Toxicology, Guangdong Province Hospital for Occupational Disease Prevention and Treatment, 68 Haikang St., Xiangang Rd. W., Guangzhou, 510300, China.

E-mail addresses: [huangzhenlie@126.com](mailto:huangzhenlie@126.com) (Z. Huang),

[wangq27@mail.sysu.edu.cn](mailto:wangq27@mail.sysu.edu.cn), [wangqing\\_gz@163.com](mailto:wangqing_gz@163.com) (Q. Wang).

<sup>1</sup> These authors contributed equally to this work.

than the safety standard of 15 mg/m<sup>3</sup> (about 3.71 ppm) set by the Chinese Labor and Hygiene Department.

Many studies have shown that the nervous system tissue is the main area for 1,2-DCE accumulation and can result in lethal toxic encephalopathy (Hotchkiss et al., 2010; Wang et al., 2014). However, inhalation of 1,2-DCE can also severely impair liver function, based on data from animal models and clinical investigations. For instance, 1,2-DCE inhalation has been shown to cause elevations in serum alanine aminotransferase (ALT) with hepatomegaly, steatosis, and biochemical abnormalities in the livers of mice (Storer et al., 1984; Sun et al., 2015). Results of a previous study in humans (Cheng et al., 1999) suggested that exposure to low or moderate levels of 1,2-DCE could result in a higher risk for developing hepatic damage in occupational workers compared with those not exposed to 1,2-DCE. In general, 1,2-DCE-induced liver abnormalities may involve necrosis (Storer et al., 1984), steatosis (Freundt et al., 1977), cirrhosis (Przezdzia and Bakula, 1975), and/or neoplasm (Nagano, 1998). One line of evidence has indicated that the accumulation of reactive oxygen species (ROS) (Sun et al., 2015), the impairment of macromolecules (Kitchin and Brown, 1994; Sasaki et al., 1998), and the dysfunction of the hepatocellular metabolism (Cottalasso et al., 1994a) might underlie the above hepatic toxic effects. Nevertheless, the molecular mechanism(s) responsible for the hepatic abnormalities induced by 1,2-DCE have yet to be clarified.

## 2. Materials and methods

### 2.1. Chemicals and reagents

1,2-DCE, chloroethanol, chloroacetaldehyde, and 2-CA (chromatographic grade) were purchased from Guangzhou chemical reagent factory (Guangzhou, China). TaqMan® Gene Expression Assays and 2 × TaqMan® Gene Expression Master Mix were purchased from Applied Biosystems (Foster City, CA, USA). The primers used for mRNA qRT-PCR were purchased from Generay Biotechnology (Shanghai, China). The antibodies against mouse PYGL (1:1000), G6PC (1:1000), and β-actin (1:10,000) were purchased from Proteintech Group (Rosemont, IL, USA). The antibodies against Akt1 (1:2000) and phospho-Akt1 (Ser473) (1:2000) were purchased from Abcam (Cambridge, UK).

### 2.2. Animals

According to preliminary experimental results, male mice were more sensitive to 1,2-DCE exposure (Supplementary data, Table S1). Thus, a total of 30 National Institutes of Health (NIH) Swiss male mice (specific pathogen free, 7 weeks old, body weight 18–20 g) were purchased from Guangdong Medical Laboratory Animal Center (Guangzhou, China). All mice were housed and acclimated to the new environment for 1 week, in a temperature (23–25 °C) and humidity (50–60%) controlled room under a 12 h

light/dark cycle (lights on at 8:00 a.m. and off at 8:00 p.m.). The mice were then randomly divided into three groups of 10 mice each. Food and sterilized water were provided *ad libitum*. The study protocol was approved by the Scientific Research Committee on Ethics in the Care and Use of Laboratory Animals of Guangdong Province Hospital for Occupational Disease Prevention and Treatment (Permit No. 2015-06) and was conducted according to the NIH guidelines concerning the protection and control of animals. The histopathological, transcriptomic, and the biochemical analyses were performed using the left lateral lobes of the mouse livers.

### 2.3. 1,2-DCE inhalation exposure and quality control

The median lethal concentration (LC<sub>50</sub>) of 1,2-DCE, administered by inhalation, was estimated to be 1324.00 mg/m<sup>3</sup> for the male NIH Swiss mice (95% confidence interval: 919.92–1905.58 mg/m<sup>3</sup>) and was based on our preliminary experimental results (Supplementary data, Table S1). Therefore, concentrations of 700 mg/m<sup>3</sup> (approximately 1/2 LC<sub>50</sub>) and 350 mg/m<sup>3</sup> (1/4 LC<sub>50</sub>) 1,2-DCE were selected for the following 28 consecutive day (6 h/day) inhalation exposure experiment. 1,2-DCE aerosol was generated using a Permeacal Permeater (PD-1B, GASTEC CORP, Ayase, Japan) connected to a dry air filter, as the carrier gas, in a 300 L compressed gas cylinder and was put into glass, whole body, dynamic inhalation chambers (Guangzhou JIUFANG Electronics Co., Ltd, Guangzhou, China). These chambers allowed for automatic, dynamic 50 L/min air recycling. During the 28-day exposure period, the 1,2-DCE concentration was monitored at least three times per day (2 h/time) on the first, third, and fifth hour, in the two exposure groups (350 and 700 mg/m<sup>3</sup>) and one time per day at the last hour, in the control group. Air samples from each chamber were collected using an active carbon tube (Nantong Jinnan Glass and Equipment Co., Jiangsu, China) connected to an air sampler (50 m<sup>3</sup>/h, Gilian LFS-113DC, Sensidyne, St. Petersburg, FL, USA) and analyzed by gas chromatography-mass spectrometry (GC-MS) (6890N gas chromatograph, 5957 Mass Selective Detector, 7683 Automatic Liquid Sampler; Agilent Technologies, Santa Clara, CA, USA). The air sample results were then averaged over 28 days to obtain the mean and standard deviation values.

During exposure, other quality control data, including temperature, humidity, oxygen levels and carbon dioxide and aerosol particle size in the chambers were monitored by an RAE MultiRAE Lite Gas and VOC monitor (RAE Gas Detection systems, North Little Rock, AR, USA) and a scattered-light aerosol spectrometer system (Palas Promo 2000, Palas GmbH, Karlsruhe, Germany). The majority indexes of atmospheres in different chambers were consistent: more than 90% of the aerosol particles in the 1,2-DCE exposure chambers were less than or nearly equal to 1.5 μm as evidenced by the fact that the aerosolized 1,2-DCE particles were transported to the lung bronchi of mice via inhalation. Detailed information of exposures and quality control data are shown in

**Table 1**  
Environmental parameters of the 1,2-DCE-inhalation exposure chamber.

	Control group	350 mg/m <sup>3</sup> 1,2-DCE group	700 mg/m <sup>3</sup> 1,2-DCE group
1,2-DCE in air (mg/m <sup>3</sup> )	0.27 ± 0.11	363.58 ± 24.76**	731.10 ± 158.44**
Urine 2-CA (μg/L)	2.87 ± 0.97	1247.93 ± 258.96**	1906.5 ± 639.19**
Diameter of 90% particle (μm)	1.05	0.92	1.43
T (°C)	22.98 ± 3.06	23.26 ± 3.05	23.75 ± 3.03
H (%)	62.65 ± 10.32	61.68 ± 10.82	63.34 ± 10.22
Oxygen (%)	20.09 ± 0.00	20.32 ± 0.20	20.22 ± 0.10
Carbon dioxide (%)	0.54 ± 0.13	0.53 ± 0.08	0.56 ± 0.10

Note: T: temperature; H: humidity; \*\*P < 0.01, significantly different from the control group.

**Table 1.** The body weights of mice in each group and any toxic effects were recorded daily, during exposure. None of the mice died during the 1,2-DCE exposure period. At the end of the experiment, mice were euthanized within 24 h after the last exposure. All mice were fasted for 12 h prior to sacrifice. The organs were excised, frozen in liquid nitrogen and stored at  $-80^{\circ}\text{C}$ . Approximately 500  $\mu\text{L}$  of serum was collected and stored at  $-80^{\circ}\text{C}$  until analysis of serum parameters.

#### 2.4. Blood and liver biochemical analysis

Serum Aspartate aminotransferase (AST) and ALT levels were measured using a CL-8000 Clinical Chemistry Analyzer (Shimadzu Co., Kyoto, Japan). Serum glucose and triglyceride (TG) levels were determined using a glucose oxidase/peroxidase method and enzymatic colorimetric method, respectively. Serum FFA was determined using a non-esterified free fatty acid assay kit (Nanjing Jiancheng, Nanjing, China). Hepatic glycogen content was measured using an anthrone-sulfuric acid method (Lu et al., 2012). FFA and TG in mouse livers were tested using commercial kits from Nanjing Jiancheng Bioengineering Institute (Nanjing, China). Urine 2-chloroethanol, 2-chloroacetaldehyde, and 2-CA were assayed by GC-MS.

#### 2.5. Histopathological examination

At the end of the experiment, part of the left lateral lobes of mouse livers were removed and rinsed with cold saline. After overnight fixation in 4% paraformaldehyde, liver tissues were embedded in paraffin, and 4  $\mu\text{m}$  sections were collected and stained with hematoxylin-eosin (H&E) or Periodic Acid-Schiff (PAS). Additionally, liver slices were incubated with anti-F4/80 antibody for detection of inflammation. For Oil Red O staining, liver tissues, which were frozen in optimal cutting temperature (OCT) compounds, were sliced at 10  $\mu\text{m}$ . The frozen slices were dried for 10 min at  $25^{\circ}\text{C}$  and stained for 1 h in Oil Red O solution. Nuclei were stained with Meyer's hematoxylin solution. Evaluation of the liver slices was conducted using a light microscope (Axiphot, Carl Zeiss, Dublin, CA, USA). Intralobular degeneration and focal necrosis, glycogen and lipid accumulation, and portal inflammation were compared across groups.

#### 2.6. Gene expression microarray

The Agilent Whole Mouse Genome 4\*180K Microarray (Agilent Technologies, Santa Clara, CA, USA) was used by Shanghai OE Biotech Co., Ltd (Shanghai, China) to detect alterations in gene expression in RNA samples collected from three control mice and three 700 mg/m<sup>3</sup> 1,2-DCE-treated mice. Microarray slides were scanned using an Agilent scanner and output images were digitalized using Feature Extraction software (Agilent Technologies). The raw data were normalized with GeneSpring software (version 12.0, Agilent Technologies) using quantile normalization, according to the procedures recommended by Agilent Technologies. Differentially expressed genes were identified through absolute fold change  $>= 2.0$  as well as  $P$  value  $<= 0.05$  calculated with *t*-test.

#### 2.7. Bioinformatics analysis

Gene ontology (GO) and pathway analyses were performed using the database for annotation, visualization and integrated discovery (DAVID) program, version 6.7 (<http://david.abcc.ncifcrf.gov>) in order to identify significantly represented biological themes and functional groups in the gene list. The GO terms

and KEGG pathways with FDR-corrected  $P$  values of  $<0.05$  were considered to be enriched.

#### 2.8. Cell culture

The mouse hepatocellular cell line, AML12, was obtained from ATCC (Manassas, VA, USA). AML12 cells were cultured in Dulbecco's Modified Eagle's medium (DMEM)/F12 supplemented with 10% fetal bovine serum (FBS) and 4 mM L-glutamine and incubated at  $37^{\circ}\text{C}$  in a humidified chamber with 5% CO<sub>2</sub>. All cell culture reagents were purchased from Applied Biosystems (Waltham, MA, USA).

#### 2.9. mRNA expression analysis

Total RNA was obtained from mouse liver tissues or cultured cells using TRIzol reagent (Invitrogen, Carlsbad, CA, USA), in accordance with the manufacturer's recommendations. cDNAs were generated from total RNA using a ReverTra Ace® qPCR RT Kit (Toyobo, Tokyo, Japan). Briefly, 500 ng of RNA was reverse transcribed with Oligo (dT) primers. The reverse transcription reaction conditions were as follows: 5 min at  $65^{\circ}\text{C}$ , 15 min at  $37^{\circ}\text{C}$ , and 5 min at  $98^{\circ}\text{C}$ . Next, quantitative real-time PCR (qRT-PCR) was performed using the SYBR Green PCR Master Mix (Toyobo) with the Applied Biosystems® ViiA™ 7 Real-Time PCR kit.  $\beta$ -actin was used as an endogenous control in the cell or tissue samples. The relative expression of mRNAs was calculated using the  $2^{-\Delta\Delta C_t}$  method. Three independent experiments were performed. The primers used for qPCR are provided in Supplementary data, Table S2.

#### 2.10. Western blotting

Mouse hepatic tissues or AML12 cells were lysed in Radioimmunoprecipitation assay (RIPA) buffer containing 50 nM Tris (pH = 7.0), 0.5% SDS, 10 mM EDTA (pH = 8.0), and proteinase and phosphatase inhibitor cocktail, EDTA-free (Roche, Indianapolis, USA). Soluble proteins were obtained by centrifugation at 800  $\times g$  for 10 min to remove insoluble debris. Proteins (40  $\mu\text{g}$ ) in each sample were separated on an SDS-PAGE gel before immunoblotting.

#### 2.11. Statistical analysis

All experiments were repeated at least three times. Data are presented as mean  $\pm$  S.D. All statistical analyses were performed using SPSS 20.0 software. The differences between the three groups were analyzed using a one-way ANOVA followed by a Mann-Whitney test. Differences were considered statistically significant at  $P < 0.05$ .

### 3. Results

#### 3.1. Environmental parameters of the 1,2-DCE-inhalation exposure model

GC-MS results revealed that the actual levels of 1,2-DCE in the exposure chambers during the experiment were similar to the pre-designed 1,2-DCE concentrations. Additionally, other environmental exposure parameters were analogous in all groups, suggesting that the biological changes in mouse livers were mainly dependent on the doses of 1,2-DCE (Table 1).

#### 3.2. The general toxic effects of 1,2-DCE in mouse livers

To validate the actual inhalable efficiency of 1,2-DCE, urine 1,2-DCE metabolites (2-chloroethanol, 2-chloroacetaldehyde, and 2-

chloroacetic acid) were first examined. Urine 2-chloroacetic acid (2-CA) levels were markedly increased in both of the 1,2-DCE-exposure groups (Table 1), however, the levels of 1,2-DCE, 2-chloroethanol and 2-chloroacetaldehyde were below the detection limit (2.42 µg/L for 1,2-DCE, 3.76 µg/L for 2-chloroethanol, and 2.0 µg/L for 2-chloroacetaldehyde). Since the metabolism of 1,2-DCE to 2-CA in the liver mainly occurs through the CYP2E1 pathway, the influence of 1,2-DCE exposure on CYP2E1 expression was examined. Fig. 1A–B shows that 1,2-DCE exposure slightly increased hepatic CYP2E1 mRNA and protein expression, indicating that the abundant CYP2E1 basal expression present in the livers

of NIH Swiss mice might be sufficient to metabolize 1,2-DCE. In this study, no significant differences in food consumption were found across the groups. The average food consumption was  $254.60 \pm 35.71 \text{ g kg}^{-1} \text{ d}^{-1}$  in the control group,  $242.00 \pm 22.02 \text{ g kg}^{-1} \text{ d}^{-1}$  in the  $350 \text{ mg/m}^3$  1,2-DCE exposure group and  $243.00 \pm 37.88 \text{ g kg}^{-1} \text{ d}^{-1}$  in the  $700 \text{ mg/m}^3$  1,2-DCE exposure group ( $P=0.931$ ). The body weights of mice in each group increased gradually; however, a significant loss in body weight was observed on the 28th day in mice in the  $700 \text{ mg/m}^3$  1,2-DCE-exposure group compared with mice in the control group (Fig. 1C). The body weight gain in the control group, the  $350 \text{ mg/m}^3$  1,2-DCE

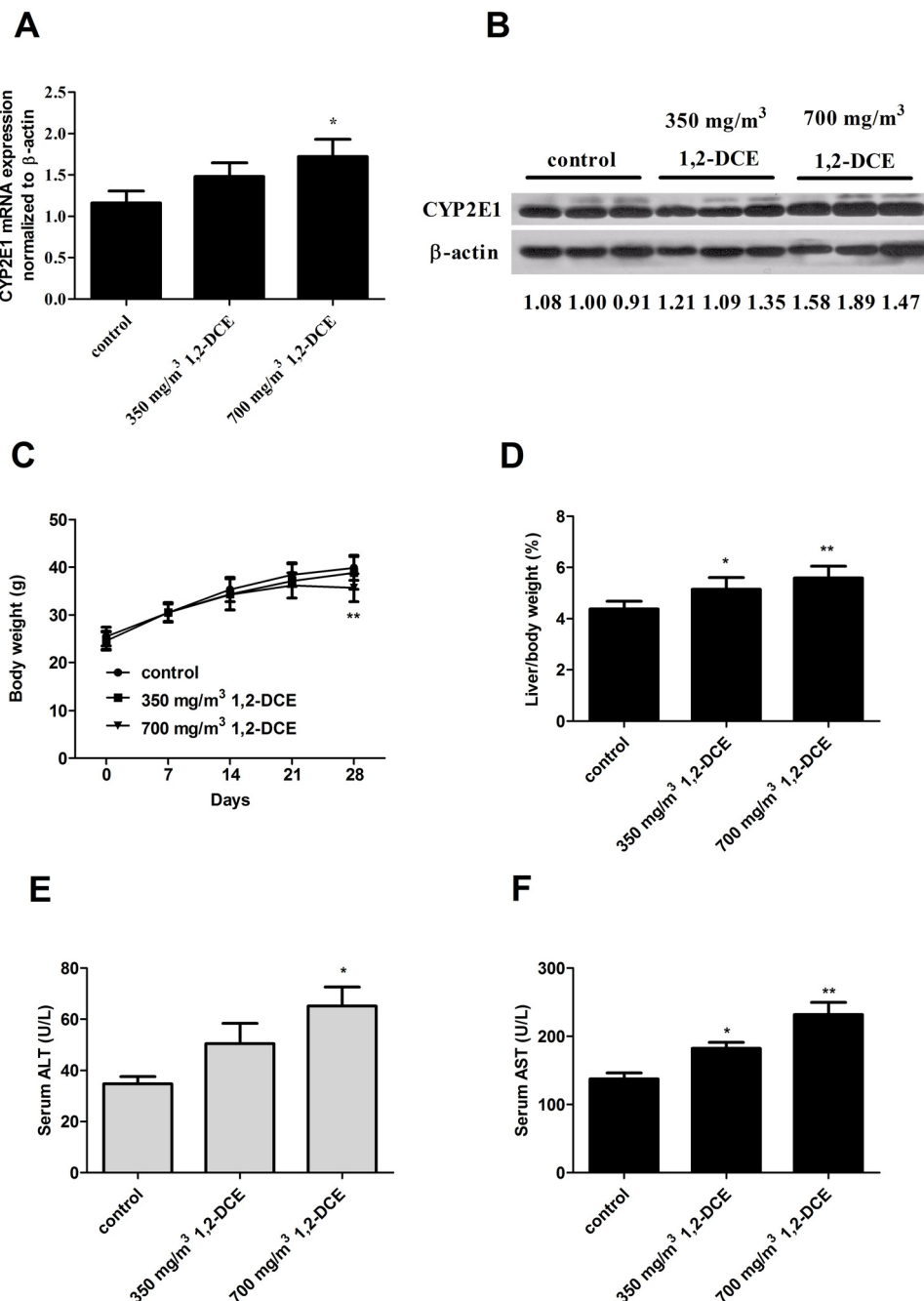


**Fig. 1.** Effects of 1,2-DCE exposure on hepatic CYP2E1 expression, body weight, liver/body weight ratios, ALT, and AST in male NIH Swiss mice. (A) mRNA expression of CYP2E1 was examined by qRT-PCR using specific primers. β-actin was used as the endogenous control. The mRNA levels represent relative values compared to the control group. (B) CYP2E1 protein expression was examined by western blot. β-actin was used as the endogenous control. The protein levels represent relative values compared to the control group. (C) Mean body weights of male mice treated with 1,2-DCE or fresh air in the whole-body exposure chamber on d7, d14, d21 and d28 are presented as the mean  $\pm$  SD. (D) Liver/body weight ratios (%) in male mice exposed to 1,2-DCE or fresh air for 28 days. Data are shown as mean  $\pm$  SD. (E–F) The sera biochemical parameters of liver function (AST and ALT) were detected. Data are shown as mean  $\pm$  SD for three groups. \* $P < 0.05$ , \*\* $P < 0.01$ , compared with the control group.

exposure group and the 700 mg/m<sup>3</sup> 1,2-DCE exposure group was  $14.4 \pm 2.311$  g,  $14.25 \pm 3.424$  g, and  $10.83 \pm 3.362$  g, respectively. Mice in the 350 mg/m<sup>3</sup> 1,2-DCE and 700 mg/m<sup>3</sup> 1,2-DCE groups had significantly higher liver/body weight ratios compared with the control group (Fig. 1D). The serum biochemistry assay showed that slight, though statistically significant, changes in ALT and AST in mice exposed to 1,2-DCE when compared to control mice (Fig. 1E–F). Pathological examination of liver tissues revealed a ubiquitous incidence of the vacuole formation, which occurred in the hepatocytes of mice exposed to the 700 mg/m<sup>3</sup> 1,2-DCE and to a lesser extent in mice exposed to 350 mg/m<sup>3</sup> 1,2-DCE (Fig. 2A–C). However, infiltration of inflammatory cells (Fig. 2J–L) and necrosis foci of hepatocytes were not observed in either of the 1,2-DCE-

exposure groups. These findings demonstrate that inhalation exposure to 1,2-DCE for 28 days led to mild hepatotoxicity.

### 3.3. Glycogen, FFA and triglyceride accumulation induced by 1,2-DCE in the livers of mice

Previous studies have indicated that exposure to 1,2-DCE and its metabolites might result in hepatic damage via disruption of glucose and lipid metabolism (Cottalasso et al., 1994; Kato-Weinstein et al., 1998; ATSDR, 2001). Therefore, the concentrations of glycogen and lipids was measured in the livers and blood of mice after 28 consecutive days of exposure to 1,2-DCE. As expected, liver glycogen, triglycerides, and FFA contents were significantly higher

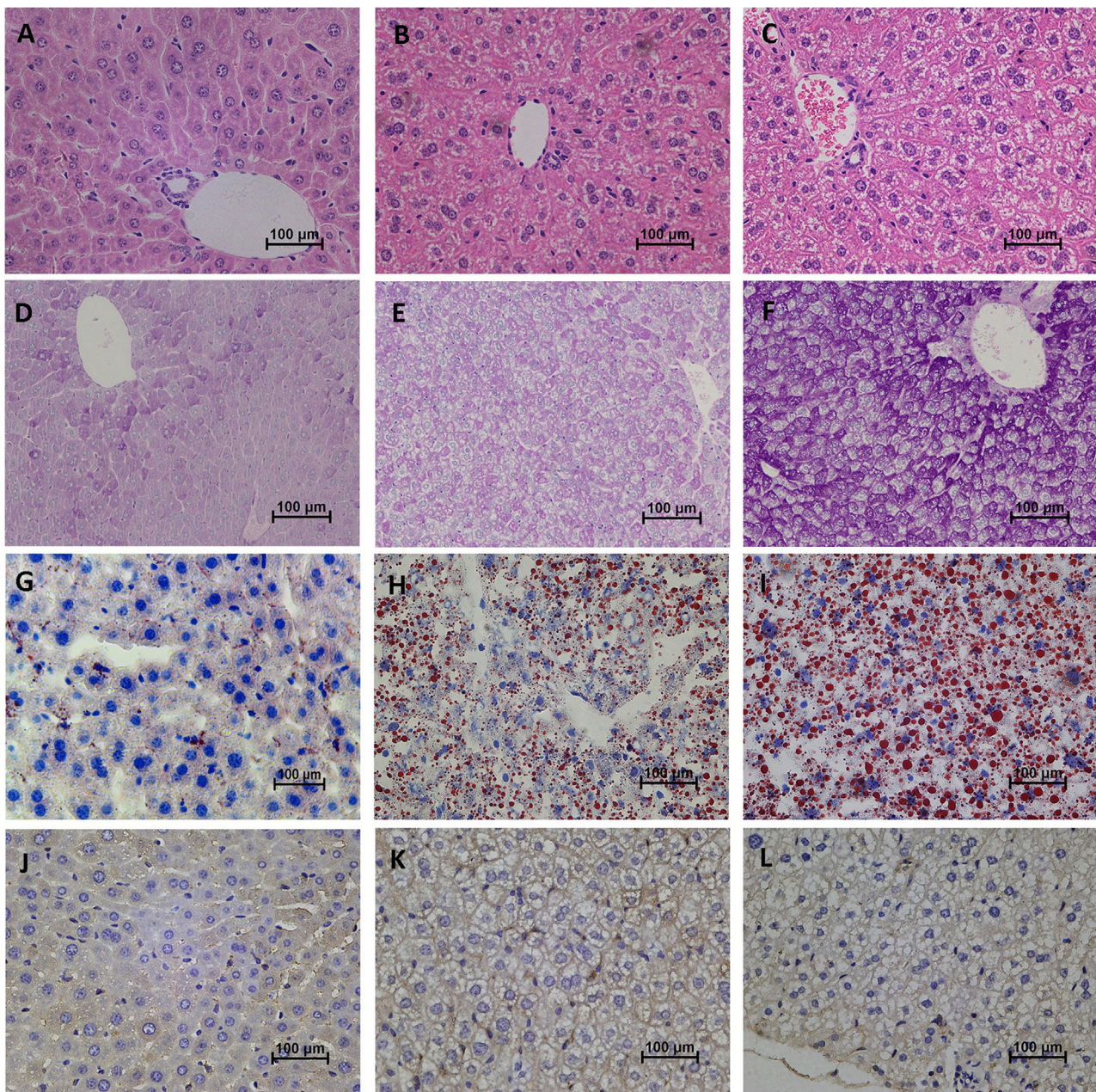


**Fig. 2.** Examination of liver histology by H&E, PAS, Oil Red O and F4/80 staining. (For interpretation of the references to colour in this figure legend, the reader is referred to the web version of this article.)

(A–C) H&E staining in liver tissues from control mouse, mouse exposed to 350 mg/m<sup>3</sup> 1,2-DCE and mouse exposed to 700 mg/m<sup>3</sup> 1,2-DCE; (D–F) PAS staining of glycogen granulation in liver tissues from control mouse, mouse exposed to 350 mg/m<sup>3</sup> 1,2-DCE and mouse exposed to 700 mg/m<sup>3</sup> 1,2-DCE; (G–I) Oil Red O staining of lipid droplet in liver tissues from control mouse, mouse exposed to 350 mg/m<sup>3</sup> 1,2-DCE and mouse exposed to 700 mg/m<sup>3</sup> 1,2-DCE; (J–L) F4/80 staining of macrophage in liver tissues from control mouse, mouse exposed to 350 mg/m<sup>3</sup> 1,2-DCE and mouse exposed to 700 mg/m<sup>3</sup> 1,2-DCE.

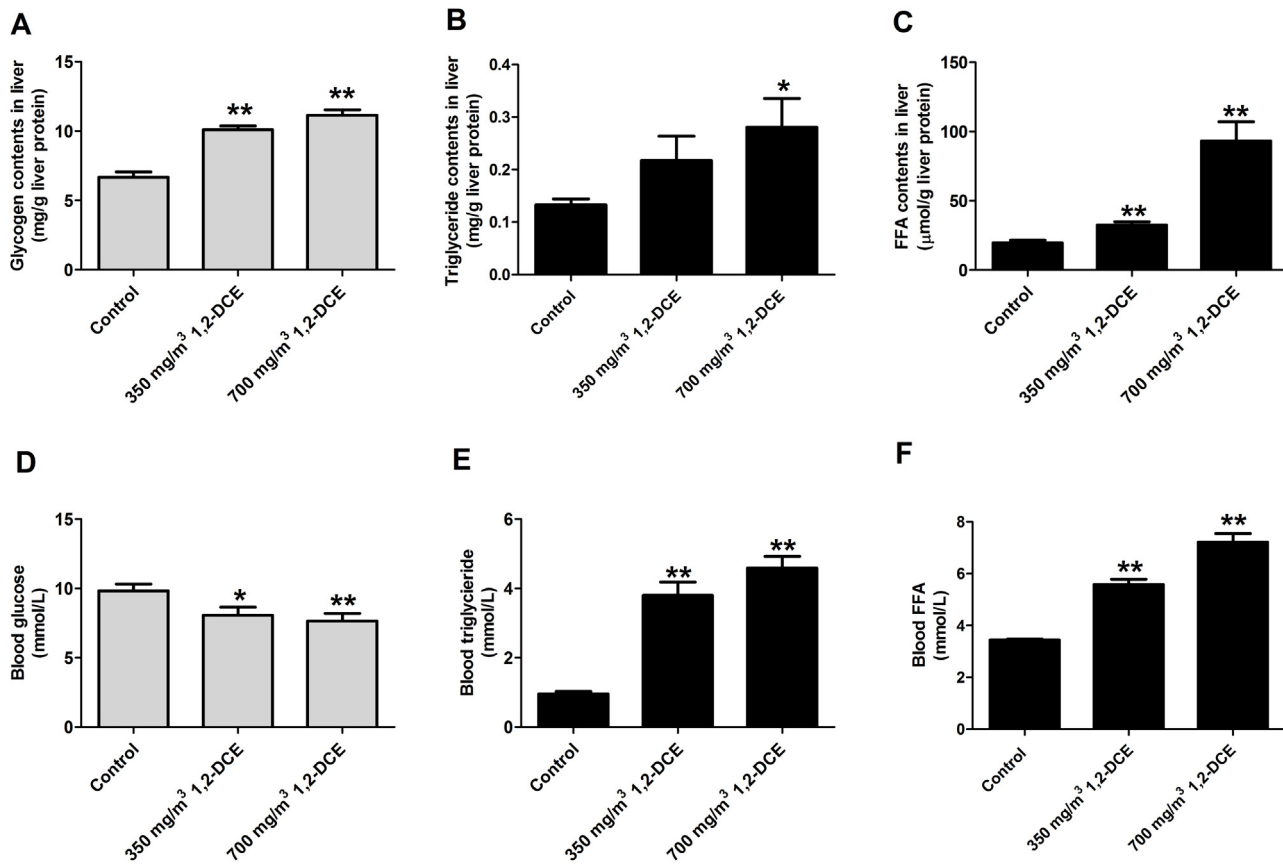


**Fig. 3.** Glycogen, FFA and triglyceride accumulation induced by 1,2-DCE in male mouse livers.

(A–D) Liver glycogen, triglyceride and FFA contents were detected in all mouse liver samples. (E–F) 20 μL serum from each mouse was used to assay the blood glucose, triglyceride and FFA levels. Data are shown as mean ± SD for three groups. \*P < 0.05, \*\*P < 0.01, compared with the control group.

in mice exposed to 350 mg/m<sup>3</sup> or 700 mg/m<sup>3</sup> 1,2-DCE compared to controls (Fig. 3A–D). Results of PAS and Oil Red O staining also confirmed that the accumulation of glycogen and lipids in the liver tissue was induced by 1,2-DCE in a dose-dependent manner (Fig. 2D–F; G–I). Additionally, serum biochemistry analysis showed that blood glucose levels in the 350 mg/m<sup>3</sup> and 700 mg/m<sup>3</sup> 1,2-DCE groups were decreased by 20% and 24%, respectively, compared with the control group. However, blood triglyceride and FFA levels were increased by 2.96-fold and 1.71-fold, respectively, in the 350 mg/m<sup>3</sup> 1,2-DCE group and by 3.78-fold and 2.10-fold, respectively, in the 700 mg/m<sup>3</sup> 1,2-DCE group, compared with the control group (Fig. 3E–F). These results demonstrate that exposure to 1,2-DCE for 28 days significantly disrupted hepatic glucose and lipid homeostasis.

#### 3.4. Identification of differentially expressed genes in the livers of mice exposed to 1,2-DCE

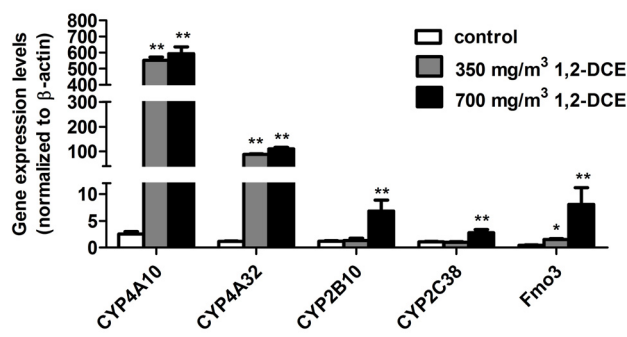
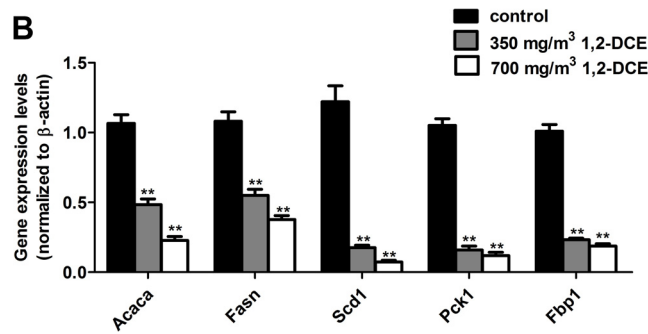
To identify global changes in hepatic gene expression and to explore the possible molecular mechanisms involved in 1,2-DCE-induced abnormalities of liver glucose and lipid metabolism, high-throughput detection, using Aligent microarray chips, was performed on three liver RNA samples from the control and three liver RNA samples from the 700 mg/m<sup>3</sup> 1,2-DCE groups. After detection, the transformed and normalized data were subjected to two-way ANOVA. After removal of unknown and repeated probe sets, statistical analysis showed a significant difference of at least 2-fold ( $P < 0.05$ ) in the expression of 689 mRNAs when comparing samples from the 700 mg/m<sup>3</sup> 1,2-DCE exposure group to the control group (Supplementary data, Table S3). Among these, 218

mRNAs were up-regulated and 471 mRNAs were down-regulated in samples from the 700 mg/m<sup>3</sup> 1,2-DCE exposure group. To verify the gene expression level found in the oligonucleotide microarray analysis, 10 genes from each mouse liver sample (five up-regulated and five down-regulated) were selected and subjected to qRT-PCR analysis. Fig. 4 shows that the altered trends of the selected gene mRNA expressions were consistent with the data from the microarray, which supports the validity of the criteria used for candidate gene screening in this study.

#### 3.5. Functional annotation of differentially expressed genes in livers of mice exposed to 1,2-DCE

The 689 differentially expressed genes were individually annotated and the predominant biological processes represented by these genes were identified using gene ontology (GO)-based enrichment analysis. Three different GO sub-ontologies including cellular component, biological process and molecular function were included in the analysis. The significantly enriched GO terms were ranked by their respective P values. Intriguingly, the analysis data of GO biological processes revealed that the 1,2-DCE-induced differentially expressed genes were mostly associated with hepatic metabolic processes. All GO analysis data are shown in Supplementary data, Table S4.

The Kyoto Encyclopedia of Genes and Genomes (KEGG) pathway annotations of the differentially expressed genes was then used to explore the possible pathways involved in 1,2-DCE-mediated liver metabolic dysfunction. A total of 20 KEGG pathways were significantly overrepresented (false discovery rate [FDR]-corrected  $P < 0.05$ ). As shown in Table S5, the top-ranked

**A****B**

**Fig. 4.** Validation of the expression of differentially expressed mRNAs in the microarray-chip using the qRT-PCR method. Quantitative real-time PCR (qRT-PCR) was performed to validate the expressions of CYP4A10, CYP4A32, CYP2B10, CYP2C38, flavin-containing monooxygenase 3 (Fmo3), acetyl-CoA carboxylase (Acaca), fatty acid synthase (Fasn), stearoyl-Coenzyme A desaturase 1 (Scd1), phosphoenolpyruvate carboxykinase 1 (Pck1) and fructose-bisphosphatase 1 (Fbp1) in all samples.  $\beta$ -actin was used as the endogenous control. The mRNA levels represent relative values compared to the control group. Data are shown as mean  $\pm$  SD for three independent experiments. \* $P < 0.05$ , \*\* $P < 0.01$ , compared with the control group.

terms also focused on liver metabolism-related pathways, such as retinol, drug, starch and sucrose metabolism. Among these differentially expressed genes, the current study initially focused on alterations in genes related to lipid metabolism because most gene clusters were enriched in lipid homoeostasis. Hepatic lipid accumulation can be caused by four different metabolic perturbations: increased hepatic *de novo* lipogenesis; increased FFA delivery to hepatocytes; decreased hepatic FFA  $\beta$ -oxidation; and inadequate TG secretion into the blood (Nagle et al., 2009). Surprisingly, the microarray data showed that the critical genes involved in FFA  $\beta$ -oxidation and TG secretion were not significantly affected by 700 mg/m<sup>3</sup> 1,2-DCE exposure, and most *de novo* lipogenesis-related genes, such as acetyl-Coenzyme A carboxylase alpha/beta (Acaca/b), fatty acid synthase (Fasn) and stearoyl-Coenzyme A desaturase 1 (Scd1), were down-regulated in mouse livers after exposure to 700 mg/m<sup>3</sup> 1,2-DCE (Fig. 4B). These data suggest that the accumulation of liver FFA and triglycerides might be due to an increased influx of circulating FFA. Peripheral tissues usually use lipids as fuel and release FFA into the blood when the blood-glucose level drops in the normal-fed state (Fig. 3D). Since hepatic glucose production is the primary mechanism regulating glucose flux in the basal state, a decrease in blood glucose levels indicates that 1,2-DCE exposure probably interrupts hepatic glucose production. Therefore, the expression of genes associated with hepatic glucose metabolism was subsequently examined. Interestingly, G6PC and PYGL (the rate-limiting enzymes of glycogenolysis) were markedly down-regulated according to the

microarray data and glycogen synthesis-related genes, such as glucokinase (Gck), hexokinase 1 (HK1), glycogen synthase kinase 3 beta (GSK3b), were unchanged. These results indicate that defective glucose generation in hepatocytes after 1,2-DCE exposure might be a potential mechanism underlying the impairment of hepatic glucose and lipid homeostasis. Hence, G6PC and PYGL mRNA and protein expressions were subsequently assayed in all mouse livers. As shown in Fig. 5A–B, the G6PC and PYLC mRNA levels in mouse liver tissues were inhibited by 46% and 64%, respectively, in the 350 mg/m<sup>3</sup> 1,2-DCE exposure group and by 69% and 68%, respectively, in the 700 mg/m<sup>3</sup> 1,2-DCE exposure group compared to the control group. G6PC, and PYGL protein expressions were also suppressed in a dose-dependent manner, compared to controls, which is consistent with the decreases observed in G6PC and PYGL mRNA levels (Fig. 5C–D). Since G6PC and PYGL are down-stream targets that are inhibited by Akt1 phosphorylation and activation (Nakae et al., 2001; Sun et al., 2016), total Akt1 (t-Akt1) protein and Akt1 (p-Akt1) phosphorylation levels were examined in mouse livers. The t-Akt1 protein levels were not affected in the livers of mice exposed to 350 mg/m<sup>3</sup> or 700 mg/m<sup>3</sup> 1,2-DCE, however, p-Akt1 levels were significantly increased by 1,2-DCE treatment.

### 3.6. The impact of 1,2-DCE and 2-CA on the expression of Akt1, G6PC, and PYGL and on the accumulation of glycogen in mouse AML12 cells

To the best of our knowledge, there have been no previous reports indicating that 1,2-DCE can activate Akt1 protein, though recent studies have found that liver glycogen accumulation and Akt1 activation are induced by a 1,2-DCE metabolite (2-CA) or chloroacetate compounds (Kato-Weinstein et al., 1998; Lingohr et al., 2002; Shahrzad et al., 2010). However, in the current study, it was unclear whether the excessive hepatic glycogen storage observed in the animal model was caused by 1,2-DCE or by metabolites of 1,2-DCE. Since CYP enzyme activity in hepatic cell lines is substantially lower compared to that of primary hepatocytes (5–15% of primary hepatocytes), 1,2-DCE- or CA-mediated alterations in glycogen accumulation, G6PC and PYGL expression levels were determined in the AML12 cell line. AML12 cells treated for 48 h with increasing concentrations of 2-CA displayed apparent decreases in the levels of G6PC and PYGL mRNA and protein expression, along with an increase in p-Akt1. Decreases in G6PC and PYGL mRNA and protein expression were concentration-dependent, reaching maximum reductions of approximately 87% and 55%, respectively, for mRNA expression and 74% and 42%, respectively, for protein expression after treatment with 50  $\mu$ M 2-CA (Fig. 6C–D). However, 1,2-DCE effects on hepatocellular G6PC and PYGL expression and Akt1 phosphorylation were not observed in this study (Fig. 6A–B). In the same experiment, AML12 cells were treated for 48 h with increasing concentrations of solvent control (DMSO), 1,2-DCE, or 2-CA. An increase in glycogen storage was observed in the 2-CA treatment group (Fig. 6F), however there was no dose-related effect on hepatocellular glycogen content found in the 1,2-DCE treatment group (Fig. 6E). These findings demonstrate that the hepatic glycogen accumulation observed in the 1,2-DCE inhalation exposure mouse model was likely due to its metabolite (2-CA)-induced Akt1 phosphorylation and activation.

## 4. Discussion

The mechanism of 1,2-DCE-induced hepatotoxicity has been attracting increasing interest from researchers. Several previous studies concerning 1,2-DCE hepatotoxicity focused on oxidative stress (Cottalasso et al., 1994b; Watanabe et al., 2007; Sun et al., 2015) and it has been suggested that the CYP2E1 pathway is

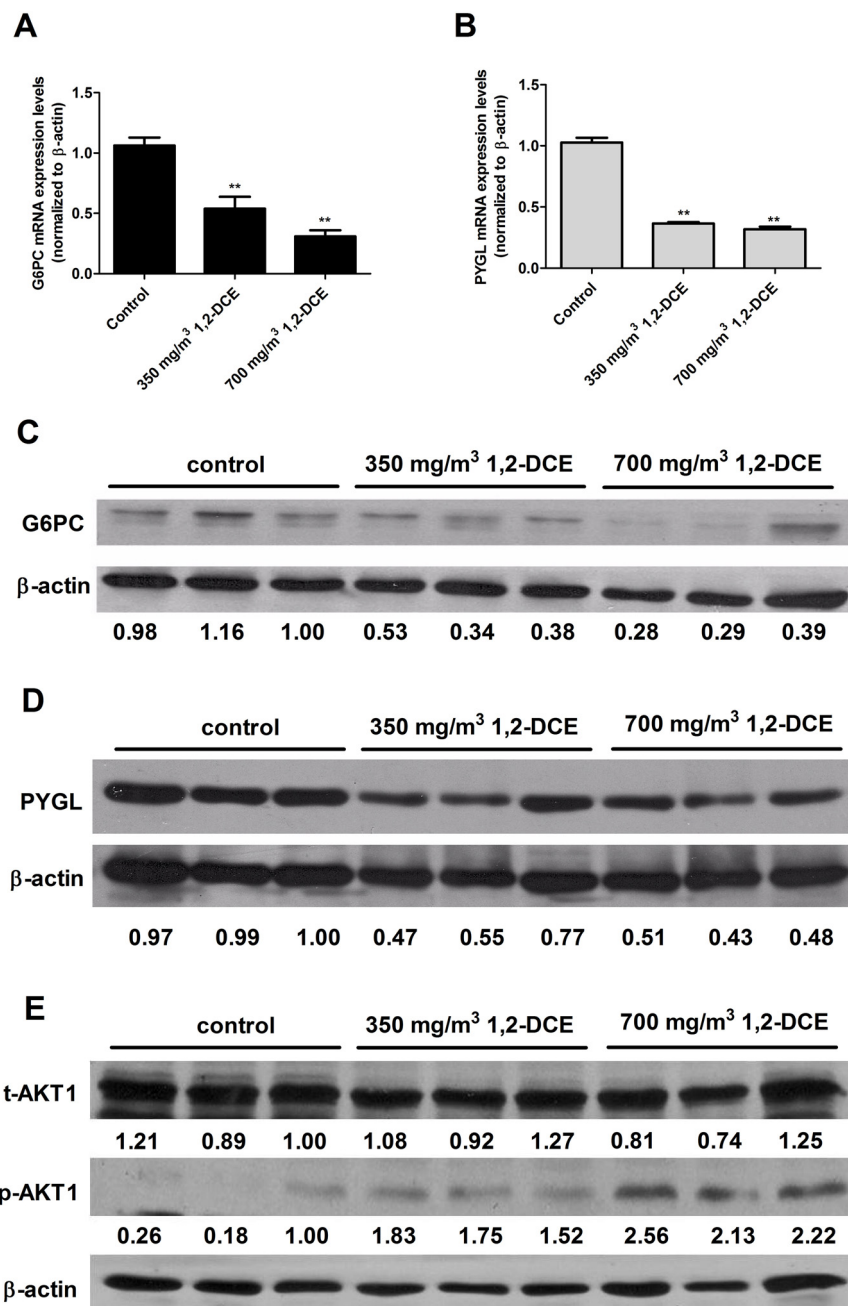


**Fig. 5.** The regulatory effects of 28-days inhalation exposure to 1,2-DCE on hepatic Akt1, G6PC and PYGL expression in male NIH Swiss mice. (A–B) Total RNA was isolated from mouse livers using TRIzol reagent. The mRNA expressions of G6PC and PYGL were then detected by qRT-PCR using specific primers.  $\beta$ -actin was used as the endogenous control. The mRNA levels represent relative values compared to the control group. Data are shown as mean  $\pm$  SD for three groups. \*\* $P < 0.01$ , compared with the control group. (C–E) Total proteins were isolated from three mouse livers in each group. The expression levels of G6PC, PYGL, t-Akt1 and p-Akt1 were assayed by Western blotting.  $\beta$ -actin was used as the endogenous control. In a representative immunoblotting image, the value under each band indicates the fold change of protein expression relative to one of the control mice.

involved in these processes. Although the current study found that 1,2-DCE exposure could induce CYP2E1 mRNA and protein expression in mouse livers, the increments in CYP2E1 expression induced by 1,2-DCE were relatively mild compared to those found in a previous study (Sun et al., 2015). Other studies have indicated that repetitive periods of hypoxia and reoxygenation can lead to an increased production of reactive oxygen species (ROS), which is a common phenomenon in cancer cells (Hsieh et al., 2010; Chen et al., 2015a, 2015b). The difference in the results obtained in this study could be due to the fact that a whole-body exposure chamber with a dynamic air-flow apparatus was used. This method avoids the hypoxia, which occurs when using the static exposure method.

Several previous animal studies have shown that 1,2-DCE exposure can lead to increases in weight and steatosis in animal livers (Storer et al., 1984; ATSDR, 2001). In this study, higher liver/body weight ratios and triglyceride accumulations in mouse livers were also consistently observed after 28 consecutive days of exposure to 1,2-DCE. Steatosis occurs when the rate of import or synthesis of fatty acids by hepatocytes exceeds the rate of export or catabolism (Bradbury and Berk, 2004). In this study, exposure to 1,2-DCE induced hepatic steatosis but inhibit the FFA *de novo* synthesis-related gene expression (Fig. 4). This might be due to 1,2-DCE-induced hypoglycemia and inactivation of the carbohydrate responsive element binding protein (ChREBP) (Dentin et al., 2005;

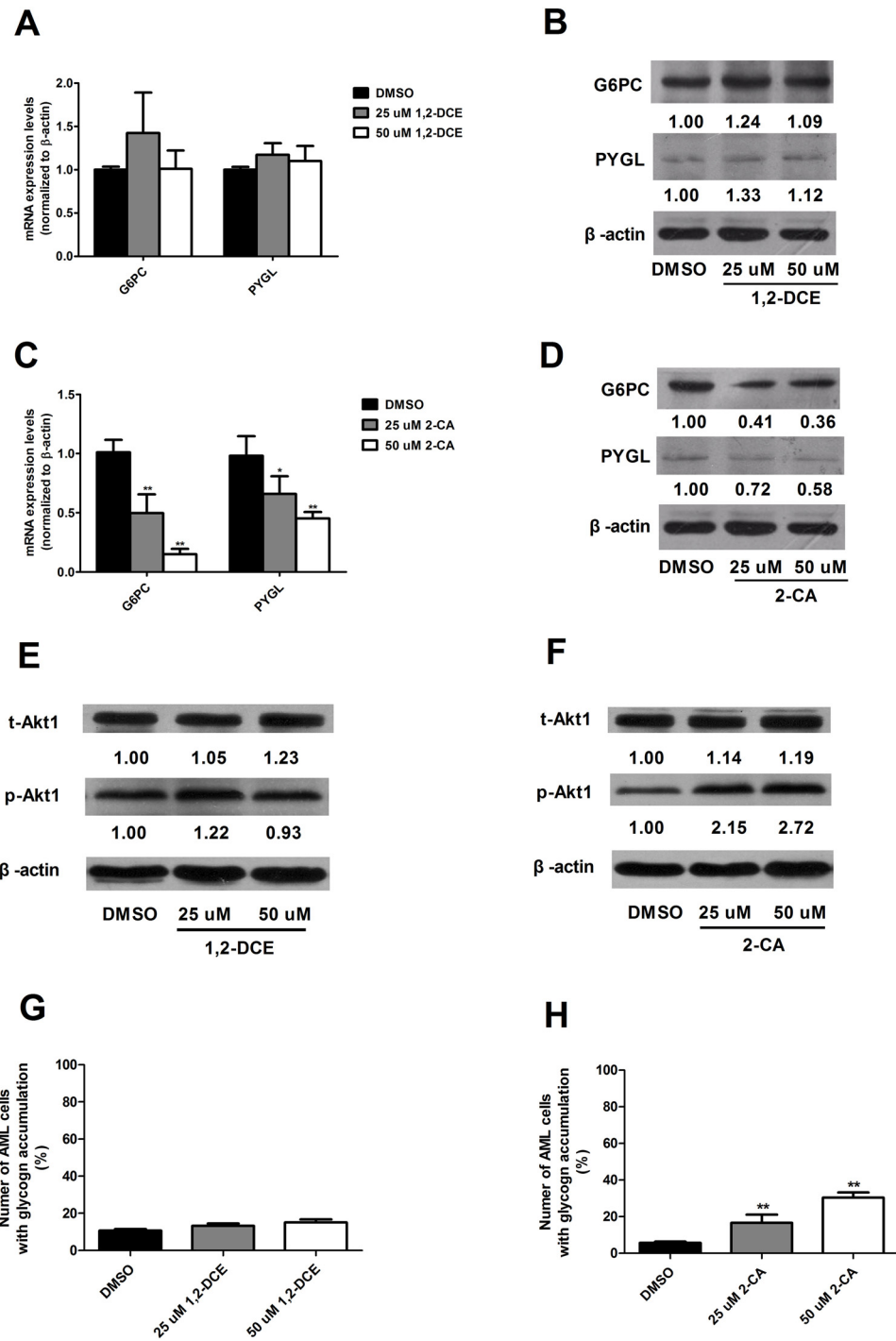


**Fig. 6.** The regulatory effects of 1,2-DCE and 2-CA on t-Akt1, p-Akt1, G6PC and PYGL expression and glycogen content in AML12 cells. The mRNA and protein expression of G6PC and PYGL were detected in 1,2-DCE-exposed AML12 cells (A-B) or 2-CA-treated cells (C-D) by qRT-PCR and Western blotting. The expression levels of t-Akt1 and p-Akt1 were detected in 1,2-DCE-exposed AML12 cells (E) or 2-CA-treated cells (F) by Western blotting.  $\beta$ -actin was used as the endogenous control for mRNA and protein. The mRNA levels represent relative values compared to DMSO-treated cells. Data are shown as mean  $\pm$  SD for three independent experiments. \* $P < 0.05$ , \*\* $P < 0.01$ , compared to cells treated with DMSO. In a representative immunoblotting image, the value under each band indicates the fold change in protein expression relative to DMSO-treated cells. (G-H) The impact of 1,2-DCE and 2-CA on glycogen content in AML12 cells. Number of AML cells with glycogen accumulation, out of 500 cells in each sample, is calculated. Data are shown as mean  $\pm$  SD for three independent experiments. \*\* $P < 0.01$ , compared to cells treated with DMSO.

(Guinez et al., 2011). Moreover, exposure to 1,2-DCE didn't influence  $\beta$ -oxidation of FFA and FFA export processes based on analysis of the microarray data. Therefore, the accumulation of hepatic lipids might be due to the increasing influx of circulating FFA into the mouse liver. The dose-dependent elevation of plasma FFA after 1,2-DCE treatment was indeed observed in this study. Additionally, a previous study (Piper et al., 2010) reported that fatty acids and

fatty acid derivatives could function as PPAR $\alpha$  ligands to activate the PPAR $\alpha$  pathway, which was also observed in the current study (Table S5). Release of FFA into blood from the peripheral tissues, also known as fat mobilization, usually occurs when the blood-glucose level drops. The significant loss in body weight of mice in the 700 mg/m<sup>3</sup> 1,2-DCE exposure group (Fig. 1C) provides indirect evidence for fat mobilization.

Hepatic glucose production is a major source for maintaining the blood-glucose level, besides the intake of exogenous carbohydrates. A decrease in blood glucose level indicates that 1,2-DCE exposure probably interrupts hepatic glucose production. In this study, persistent inhalation exposure to 1,2-DCE markedly augmented glycogen storage in livers and hampered blood glucose levels in mice. To the best of our knowledge, this is the first time this has been reported. Liver glycogen metabolism includes glycogen synthesis and glycogen degradation. Based on analysis of microarray chip results, the decreases in G6PC and PYGL (starch and sucrose metabolism pathway) mRNA expressions were intriguing because they are the rate-limiting enzymes for glycogenolysis. Much evidence (Chou et al., 2010; Froissart et al., 2011; Rubarth, 2012) has proven that loss of G6PC function leads to a decreased ability of the liver to convert G6P to glucose, resulting in glycogen accumulation and conversion to TG (Bruni et al., 1999; Chou and Mansfield, 2008). Additionally, a deficiency in glycogen phosphorylase, such as PYGL in the liver, also leads to similar clinical symptoms, known as glycogen-storage disease type VI (Chang et al., 1998; Manzia et al., 2011). Consistent with this research, a tight connection between 1,2-DCE-mediated suppression of G6PC and PYGL mRNA and protein levels with glycogen accumulation in hepatocytes was confirmed in the animal model in the current study (Fig. 4).

G6PC and PYGL genes have been proven to be negatively regulated by Akt1 phosphorylation and activation (Nakae et al., 2001; Sun et al., 2016). In this study, the phosphorylation levels of Akt1 in mice livers were remarkably increased in the 1,2-DCE exposure group, along with inactivation of G6PC and PYGL transcription. In addition to the G6PC and PYGL genes, two other Akt1-regulated genes, phosphoenolpyruvate carboxykinase 1 (*Pck1*) and fructose-bisphosphatase 1 (*Fbp1*), were also inhibited at the transcriptional level in the mouse livers after 1,2-DCE

exposure (Fig. 4B). The current *in vitro* study further proved that treatment with the 1,2-DCE metabolite (2-CA) could induce an increase in Akt1 phosphorylation level and a decrease in G6PC and PYGL expression. Interestingly, a previous study (Ono et al., 2003) also found that continuous over-expression of Akt1 in mouse livers could lead to marked hypoglycemia, hypertriglyceridemia and fatty liver. Thus, higher glycogen and lipid stored in mouse livers exposed to 1,2-DCE could be due to a disorder in hepatic glucose production, probably through activation of the Akt1 pathway and inhibition of G6PC and PYGL expression.

Previous studies have reported that 1,2-DCE is mainly metabolized by phase I metabolic enzymes and converted to 2-chloroethanol, 2-chloroacetaldehyde, and 2-CA (Guengerich et al., 1980; Reitz et al., 1982). Based on the GC-MS detection results in this study, 2-CA seemed to be the most dominant metabolite of 1,2-DCE since the levels of 2-chloroethanol or 2-chloroacetaldehyde in the mouse urine were under the detection limits. Of note, some previous studies have indicated that 2-CA or mono-chloroacetate (MCA) treatment could cause hypoglycemia and glycogen accumulation in animal livers and in cultured liver epithelial cells (Kato-Weinstein et al., 1998; Lingohr et al., 2002). Similar to these observations, mice treated with 1,2-DCE in this study also showed significant dysfunctions in glucose metabolism. Additionally, in the current study, the *in vitro* results showed that the increased level Akt1 phosphorylation and the decreased expressions of G6PC and PYGL were triggered by 2-CA, but not 1,2-DCE. Hence, 2-CA might be the active metabolite of 1,2-DCE and could be responsible for the 1,2-DCE induced liver dysfunction in NIH Swiss mice.

In conclusion, exposure to 1,2-DCE (350 mg/m<sup>3</sup> and 700 mg/m<sup>3</sup>) for 28 days caused slight liver damage in mice and significant glycogen and excessive lipid storage in hepatocytes. This might be mediated by down-regulation of hepatic G6PC and PYGL expression via the activation of Akt1. Furthermore, the *in vitro* results of

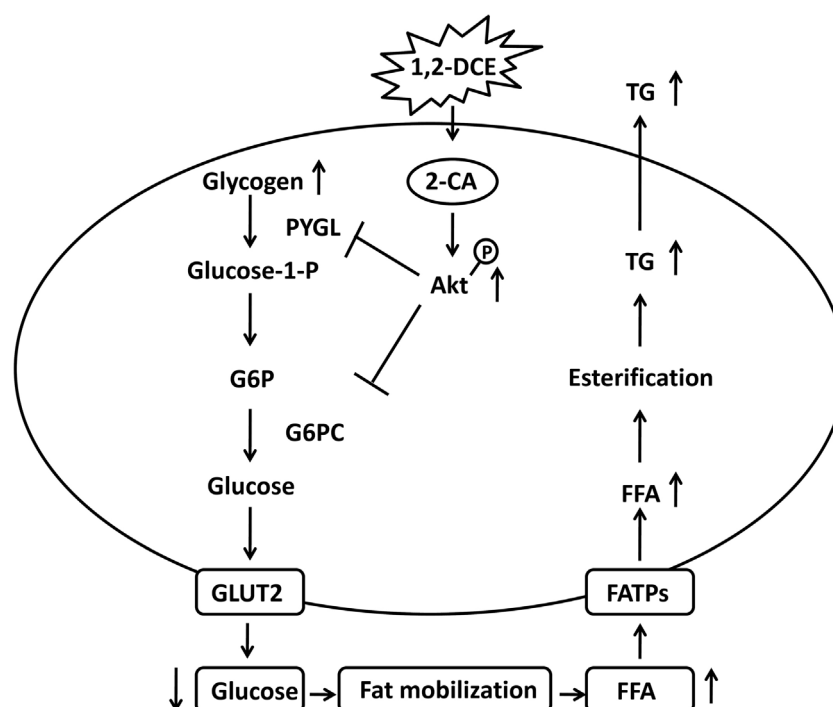


**Fig. 7.** Schematic representation of 1,2-DCE-induced impairment of glucose and lipid homeostasis. In hepatocytes, Akt1 is activated by the 1,2-DCE metabolite (2-CA). With 1,2-DCE exposure, Akt1 inhibits the expression of G6PC and PYGL and disrupts the glycogenolysis process leading to a decrease in blood glucose level. The drop in blood glucose level initiates fat mobilization and increases the level of circulating FFA; 1,2-DCE enhances hepatic TG accumulation through an increase in the influx of circulating FFA. In summary, hepatocytes exposed to 1,2-DCE, G6PC and PYGL, regulated by Akt1, are involved in the impairment of hepatic glucose and lipid homeostasis. Glucose-1-p: Glucose 1-phosphate; G6P: Glucose 6-phosphate; GLUT2: Glucose transporter 2; FATPs: FFA transporter proteins.

this study suggest that inhibition of G6PC and PYGL expression might be due to hepatic 2-CA accumulation rather than 1,2-DCE accumulation (Fig. 7).

## Conflict of interest statement

The authors declare that there are no conflicts of interest.

## Acknowledgements

This work was supported by the National Natural Science Foundations of China [grant number: 81273098, 81673140], the National Key Technology Research, Development Program of the Ministry of Science and Technology of China during the 12th Five-Year Plan Period [grant number: 2014BAI12B01], Natural Science Foundation of Guangdong Province [grant number: S2013010011816], the Guangzhou City Pearl River New Star of Science and Technology [grant number: 2013J2200020], Young teacher training Program of Sun Yat-sen University [grant number: 15ykpy06], Guangdong Provincial Key Laboratory of Occupational Disease Prevention and Treatment [grant number: 2012A061400007] and the Medical Scientific Research Foundation of Guangdong Province [grant numbers: A2012068, B2014017, B2014070, A2016137, A2016557]. We thank LetPub ([www letpub.com](http://www letpub.com)) for its linguistic assistance during the preparation of this manuscript.

## Appendix A. Supplementary data

Supplementary data associated with this article can be found, in the online version, at <http://dx.doi.org/10.1016/j.tox.2017.02.005>.

## References

- ATSDR, 2001. Toxicological Profile for 1,2-Dichloroethane. (U.S. Department, and P. H. S. Of Health And Human Services, Eds.).
- Bradbury, M.W., Berk, P.D., 2004. Lipid metabolism in hepatic steatosis. *Clin. Liver Dis.* 8, 639–671.
- Bruni, N., Rajas, F., Montano, S., Chevalier-Porst, F., Maire, I., Mithieux, G., 1999. Enzymatic characterization of four new mutations in the glucose-6 phosphatase (G6PC) gene which cause glycogen storage disease type 1a. *Ann. Hum. Genet.* 63, 141–146.
- Chang, S., Rosenberg, M.J., Morton, H., Francomano, C.A., Biesecker, L.G., 1998. Identification of a mutation in liver glycogen phosphorylase in glycogen storage disease type VI. *Hum. Mol. Genet.* 7, 865–870.
- Chen, S., Zhang, Z., Lin, H., Chen, Z., Wang, Z., Wang, W., 2015a. 1,2-Dichloroethane-induced toxic encephalopathy: a case series with morphological investigations. *J. Neurol. Sci.* 351, 36–40.
- Chen, W.L., Wang, C.C., Lin, Y.J., Wu, C.P., Hsieh, C.H., 2015b. Cycling hypoxia induces chemoresistance through the activation of reactive oxygen species-mediated B-cell lymphoma extra-long pathway in glioblastoma multiforme. *J. Transl. Med.* 13, 389.
- Cheng, T.J., Huang, M.L., You, N.C., Du, C.L., Chau, T.T., 1999. Abnormal liver function in workers exposed to low levels of ethylene dichloride and vinyl chloride monomer. *J. Occup. Environ. Med.* 41, 1128–1133.
- Chernichenko, I.A., Balenko, N.V., Litvichenko, O.N., 2009. [Carcinogenic hazard of chloroform and other drinking water chlorination by-products]. *Gig. Sanit.* 28–33.
- Chou, J.Y., Mansfield, B.C., 2008. Mutations in the glucose-6-phosphatase-alpha (G6PC) gene that cause type la glycogen storage disease. *Hum. Mutat.* 29, 921–930.
- Chou, J.Y., Jun, H.S., Mansfield, B.C., 2010. Glycogen storage disease type I and G6Pase-beta deficiency: etiology and therapy. *Nat. Rev. Endocrinol.* 6, 676–688.
- Cottalasso, D., Barisione, G., Fontana, L., Domenicotti, C., Pronzato, M.A., Nanni, G., 1994a. Impairment of lipoglycoprotein metabolism in rat liver cells induced by 1,2-dichloroethane. *Occup. Environ. Med.* 51, 281–285.
- Cottalasso, D., Barisione, G., Fontana, L., Domenicotti, C., Pronzato, M.A., Nanni, G., 1994b. Impairment of lipoglycoprotein metabolism in rat liver cells induced by 1,2-dichloroethane. *Occup. Environ. Med.* 51, 281–285.
- Dentin, R., Girard, J., Postic, C., 2005. Carbohydrate responsive element binding protein (ChREBP) and sterol regulatory element binding protein-1c (SREBP-1c): two key regulators of glucose metabolism and lipid synthesis in liver. *Biochimie* 87, 81–86.
- Freundt, K.J., Liebaldt, G.P., Lieberwirth, E., 1977. Toxicity studies on trans-1,2-dichloroethylene. *Toxicology* 7, 141–153.
- Froissart, R., Piraud, M., Boudjemline, A.M., Vianey-Saban, C., Petit, F., Hubert-Buron, A., Eberschweiler, P.T., Gajdos, V., Labrune, P., 2011. Glucose-6-phosphatase deficiency. *Orphanet J. Rare Dis.* 6, 27.
- Guengerich, F.P., Crawford, W.J., Domoradzki, J.Y., Macdonald, T.L., Watanabe, P.G., 1980. In vitro activation of 1,2-dichloroethane by microsomal and cytosolic enzymes. *Toxicol. Appl. Pharmacol.* 55, 303–317.
- Guinez, C., Filhoulaud, G., Rayah-Benhammed, F., Marnier, S., Dubuquoy, C., Dentin, R., Moldes, M., Burnol, A.F., Yang, X., Lefebvre, T., Girard, J., Postic, C., 2011. O-GlcNAcylation increases ChREBP protein content and transcriptional activity in the liver. *Diabetes* 60, 1399–1413.
- Hotchkiss, J.A., Andrus, A.K., Johnson, K.A., Krieger, S.M., Woolhiser, M.R., Maurissen, J.P., 2010. Acute toxicological and neurotoxic effects of inhaled 1,2-dichloroethane in adult Fischer 344 rats. *Food Chem. Toxicol.* 48, 470–481.
- Hou, Y., Chu, W., Ma, M., 2012. Carbonaceous and nitrogenous disinfection by-product formation in the surface and ground water treatment plants using Yellow River as water source. *J. Environ. Sci. (China)* 24, 1204–1209.
- Hsieh, C.H., Lee, C.H., Liang, J.A., Yu, C.Y., Shyu, W.C., 2010. Cycling hypoxia increases U87 glioma cell radiosensitivity via ROS induced higher and long-term HIF-1 signal transduction activity. *Oncol. Rep.* 24, 1629–1636.
- Igwe, O.J., Que, H.S., Wagner, W.D., 1986. Effect of disulfiram pretreatment on the tissue distribution macromolecular binding, and excretion of [<sup>14</sup>C]-dichloroethane in the rat. *Drug Metab. Dispos.* 14, 65–72.
- Kato-Weinstein, J., Lingohr, M.K., Orner, G.A., Thrall, B.D., Bull, R.J., 1998. Effects of dichloroacetate on glycogen metabolism in B6C3F1 mice. *Toxicology* 130, 141–154.
- Kitchin, K.T., Brown, J.L., 1994. Dose-response relationship for rat liver DNA damage caused by 49 rodent carcinogens. *Toxicology* 88, 31–49.
- Lingohr, M.K., Bull, R.J., Kato-Weinstein, J., Thrall, B.D., 2002. Dichloroacetate stimulates glycogen accumulation in primary hepatocytes through an insulin-independent mechanism. *Toxicol. Sci.* 68, 508–515.
- Liu, J.R., Fang, S., Ding, M.P., Chen, Z.C., Zhou, J.J., Sun, F., Jiang, B., Huang, J., 2010. Toxic encephalopathy caused by occupational exposure to 1,2-Dichloroethane. *J. Neurol. Sci.* 292, 111–113.
- Lu, J., Qin, J.Z., Chen, P., Chen, X., Zhang, Y.Z., Zhao, S.J., 2012. Quality difference study of six varieties of Ganoderma lucidum with different origins. *Front. Pharmacol.* 3, 57.
- Manzia, T.M., Angelico, R., Toti, L., Cillis, A., Ciano, P., Orlando, G., Anselmo, A., Angelico, M., Tisone, G., 2011. Glycogen storage disease type Ia and VI associated with Hepatocellular Carcinoma: two case reports. *Transplant. Proc.* 43, 1181–1183.
- Nagano, K.N.T.Y., 1998. Inhalation carcinogenesis studies of six halogenated hydrocarbons in rats and mice. In: Chiyotani, K., Hosoda, Y., Aizawa, Y. (Eds.), *Advances in the Prevention of Occupational Respiratory Diseases*. Elsevier, Amsterdam, pp. 741–746.
- Nagle, C.A., Klett, E.L., Coleman, R.A., 2009. Hepatic triacylglycerol accumulation and insulin resistance. *J. Lipid Res.* 50, S74–S79 (Suppl).
- Nakae, J., Kitamura, T., Silver, D.L., Accili, D., 2001. The forkhead transcription factor Foxo1 (Fkhr) confers insulin sensitivity onto glucose-6-phosphatase expression. *J. Clin. Invest.* 108, 1359–1367.
- Ono, H., Shimano, H., Katagiri, H., Yahagi, N., Sakoda, H., Onishi, Y., Anai, M., Ogihara, T., Fujishiro, M., Viana, A.Y., Fukushima, Y., Abe, M., Shojima, N., Kikuchi, M., Yamada, N., Oka, Y., Asano, T., 2003. Hepatic Akt activation induces marked hypoglycemia, hepatomegaly, and hypertriglyceridemia with sterol regulatory element binding protein involvement. *Diabetes* 52, 2905–2913.
- Pyper, S.R., Viswakarma, N., Yu, S., Reddy, J.K., 2010. PPAR $\alpha$ : energy combustion, hypolipidemia, inflammation and cancer. *Nucl. Recept. Signal.* 8, e002.
- Reitz, R.H., Fox, T.R., Ramsey, J.C., Quast, J.F., Langvardt, P.W., Watanabe, P.G., 1982. Pharmacokinetics and macromolecular interactions of ethylene dichloride in rats after inhalation or gavage. *Toxicol. Appl. Pharmacol.* 62, 190–204.
- Rubarth, L.B., 2012. Glucose-6-phosphatase and glucose-6-phosphate dehydrogenase deficiency: how are they different? *Neonatal Netw.* 31, 45–47.
- Sasaki, Y.F., Saga, A., Akasaka, M., Ishibashi, S., Yoshida, K., Su, Y.Q., Matsusaka, N., Tsuda, S., 1998. Detection of in vivo genotoxicity of haloalkanes and haloalkenes carcinogenic to rodents by the alkaline single cell gel electrophoresis (comet) assay in multiple mouse organs. *Mutat. Res.* 419, 13–20.
- Shahrzad, S., Lacombe, K., Adamcic, U., Minhas, K., Coomber, B.L., 2010. Sodium dichloroacetate (DCA) reduces apoptosis in colorectal tumor hypoxia. *Cancer Lett.* 297, 75–83.
- Storer, R.D., Jackson, N.M., Conolly, R.B., 1984. In vivo genotoxicity and acute hepatotoxicity of 1,2-dichloroethane in mice: comparison of oral intraperitoneal, and inhalation routes of exposure. *Cancer Res.* 44, 4267–4271.
- Sun, Q., Wang, G., Gao, L., Shi, L., Qi, Y., Lv, X., Jin, Y., 2015. Roles of CYP2e1 in 1,2-dichloroethane-induced liver damage in mice. *Environ. Toxicol.* 31, 1430–1438.
- Sun, Y., Guo, C.Y., Wang, D.D., Li, X.F., Xiao, L., Zhang, X., You, X., Shi, Q., Hu, G.J., Fang, C., Lin, H.R., Zhang, Y., 2016. Transcriptome analysis reveals the molecular mechanisms underlying growth superiority in a novel grouper hybrid (*Epinephelus fuscoguttatus* female symbol x *E. lanceolatus* male symbol). *BMC Genet.* 17, 24.
- Take, M., Matsumoto, M., Takeuchi, T., Haresaku, M., Kondo, H., Senoh, H., Umeda, Y., Takamura-Enya, T., Fukushima, S., 2014. Inhalation exposure to 1,2-dichloropropane: distribution of blood and tissue concentrations of 1,2-dichloropropane in rats during and after exposure. *J. Environ. Sci. Health A Tox. Hazard. Subst. Environ. Eng.* 49, 1341–1348.
- Wang, G., Yuan, Y., Zhang, J., Gao, L., Tan, X., Yang, G., Lv, X., Jin, Y., 2014. Roles of aquaporins and matrix metalloproteinases in mouse brain edema formation

- induced by subacute exposure to 1,2-dichloroethane. *Neurotoxicol. Teratol.* 44, 105–112.
- Watanabe, K., Liberman, R.G., Skipper, P.L., Tannenbaum, S.R., Guengerich, F.P., 2007. Analysis of DNA adducts formed *in vivo* in rats and mice from 1,2-dibromoethane, 1,2-dichloroethane, dibromomethane, and dichloromethane using HPLC/accelerator mass spectrometry and relevance to risk estimates. *Chem. Res. Toxicol.* 20, 1594–1600.
- Zhou, X., Zhou, W., Zhou, J., Long, L., Xiao, B., 2015. 1,2-Dichloroethane-induced toxic leukoencephalopathy with a brain biopsy. *Neurol. Sci.* 36, 817–819.